

Effect of Pt Concentration on the Grain Growth of TiO₂sol-gel Films

Y.J. Jia^{1a}, Na. An^{2b}, H.N. Chen^{3c} and Yi Chen^{4d}

¹School of Mechanical Engineering, Tianjin Polytechnic University, Tianjin 300387, China

²Siemens Mechanical Drive Systems Co., Ltd, Tianjin 300400, China

³School of Computer Science and Software Engineering, Tianjin Polytechnic University, Tianjin 300387, China

⁴Department of mechanical engineering, Inha University, 253 Yonghyun Dong, Nam Gu, Incheon, 402-751, South Korea

^ajiayanjun@tjpu.edu.cn, ^bna.an@siemens.com, ^cchenhanning@tjpu.edu.cn, ^dchenyi6970@hotmail.com

Abstract. Pt metallic has been supported on TiO₂ surface using different methods, Here, Pt doped TiO₂ (Pt-TiO₂) sol gel thin film were successfully produced by reducing chloroplatinic acid (H₂PtCl₆). The structures of prepared composites were investigated using X-ray diffraction (XRD). The physical morphologies of the composites were examined using transmission electron microscope (TEM). The grain size of Pt-TiO₂ thin film after annealing was also measured by atomic force microscope (AFM) images.

Keywords. TiO₂, Pt Annealing, Gran size

1 Introduction

Recently, extensive research for titanium dioxide (TiO₂) has been carried out in efforts to develop variety of application fields including capacitors for photovoltaic cells [1], sensors [2], antireflection films [3], white pigments [4], optical coatings [5], and high density dynamic random access memory devices [6]. TiO₂ have three different crystal phases, such as anatase, rutile, and brookite [7]. Rutile is the most common natural form of TiO₂. Brookite phase is crystallized in the orthorhombic system and exhibits no photocatalytic activity. Anatase TiO₂ has excellent photocatalytic activity, physical and chemical stabilities and antimicrobial activity [8-11].

Earlier studies have revealed that the photocatalytic activity of TiO₂ can be improved significantly by doping with noble metals such as Pt, Au, Ag, etc [12, 13]. It is well known that platinization of TiO₂ often shows a high photocatalytic activity. The doping of platinum on TiO₂ can form the Schottky diode barrier among the metals and the electronic potential barrier at the metal-semiconductor heterojunction, and the platinized TiO₂ traps the photogenerated electrons efficiently [14]. The doping of Pt on TiO₂ surface has been widely reported to improve photocatalytic performance for the split of water and the degradation of different harmful compounds [15].

In this paper, we report characteristic properties of TiO₂ and Pt composite including UV-visible spectra, transmission electron microscope (TEM) images, x-ray diffraction (XRD) patterns and atomic force microscope (AFM) images.

2 Experimental details

Titanium isopropoxide was used as a sol-gel precursor. The metal alkoxide was mixed with ethanol. The resulting solution became a milk color, and white precipitation was observed. Hydrochloric acid was slowly added to the solution with vigorous stirring until the solution become transparent. Various amounts of chloroplatinic acid (H₂PtCl₆) (8wt. % in water) was added to the TiO₂ sol-gel solution. Sodium borohydride (NaBH₄) was dispersed in ethanol and slowly added into the H₂PtCl₆/TiO₂ solution to reduce [PtCl₆]²⁻ to Pt⁰. The aged sol was spin coated onto the glass and silicon substrate by spin-coated at 2000 rpm and heated at 200 °C for 5 min.. UV-visible spectra were obtained with diode array spectrophotometer (Hewlett-Packard 8452 A). The sol-gel was diluted to ethanol and drop to the copper TEM grid. Using this copper grid sample, TEM images were obtained with CM200 (Philips) microscope. The TiO₂ thin films coated onto silicon wafer were annealed in argon environment tube furnace (EM Tech). The annealing process started from room temperature to 750°C in steps of 5 °C/min and then maintained the temperature for 1 h. The films naturally cooled down to room temperature. The TiO₂ thin films doped with Pt were subject to XRD analysis with X'Pert MPD Pro diffractometer (Philips). The surface of the film also analyzed with NanoScope 3D (Veeco) microscope.

3 Results and discussion

UV-visible spectra of bare TiO₂ and Pt-TiO₂ prepared with different Pt concentration are shown in Figure 1. The single broad intense absorption peak of Pt-TiO₂ between 300 – 350 nm can be attributed to the charge-transfer from the valence band to the conduction band. The UV-vis absorption peaks also showed a red shift due to the modification of TiO₂ with Pt [16].

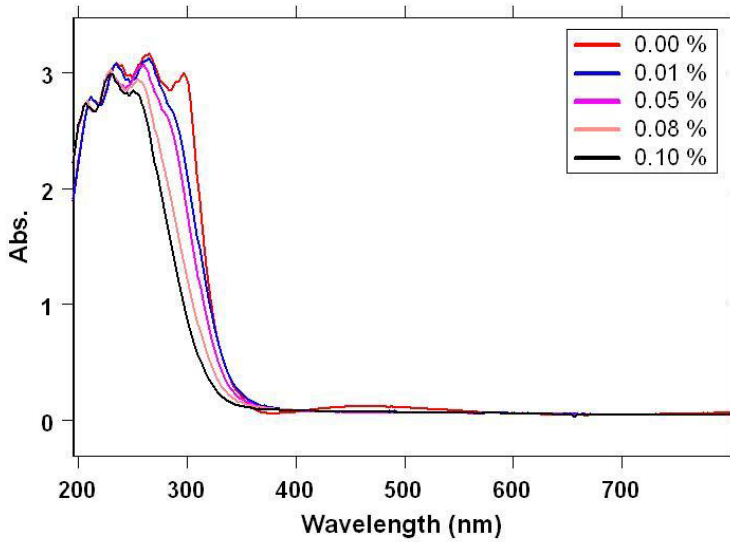


Fig. 1. UV-Visible spectra of bare TiO₂ and Pt-TiO₂ sol-gel thin film after annealing.

The UV-visible spectra show the possible uniform distribution of the Pt-nanoparticles throughout the sol-gel films. To obtain the particle size and distribution, the TEM was employed. Figure 2 (a) shows the TEM image for the 0.1% of Pt-TiO₂ film with scale bar size of 100. The aggregated area was further focused and obtained the image with scale bar size of 20 nm as shown in Figure 2 (b). Pt-nanoparticles do not have big aggregates, distribute relatively uniformly, and distribute particle sizes between 4–8 nm.

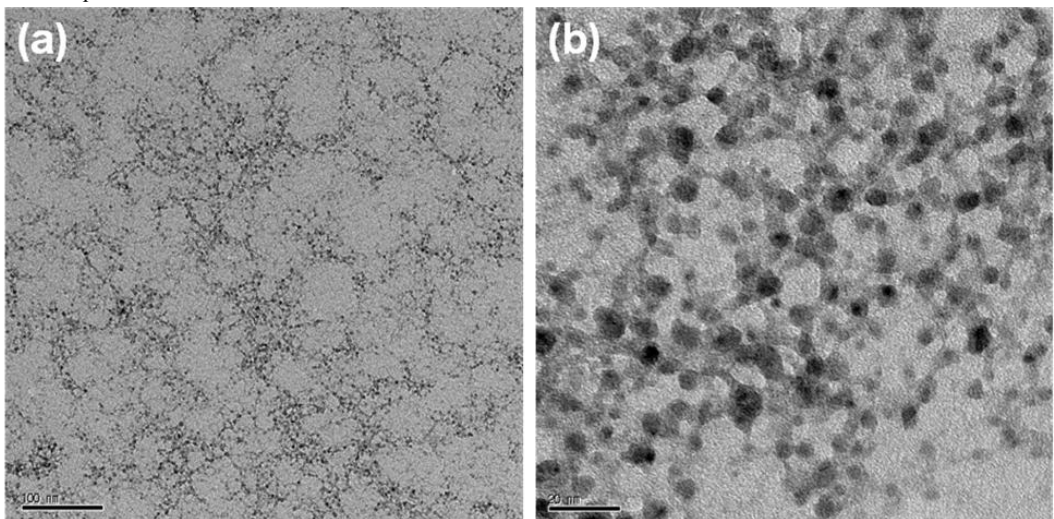


Fig.2. TEM image of TiO₂-Pt with 0.1% Pt.

Figure 3 (a) shows XRD patterns for Pt-TiO₂ films prepared by sol-gel method with various amount of Pt. All these samples show typical TiO₂ diffraction peaks in form of anatase. It shows almost coincide with a pure TiO₂ diffraction peaks and shows no diffraction peaks due to the doped Pt. It can be assumed that the amount of Pt doped particle was very low, which resulted in non-appearance of the Pt crystalline peaks [17,18]. However, diffraction intensity increased with the increase of Pt concentration. The crystalline size of the Pt-TiO₂ samples after annealing were estimated from line broadening using Scherrer equation based on (101) peak of anatase TiO₂ [19].

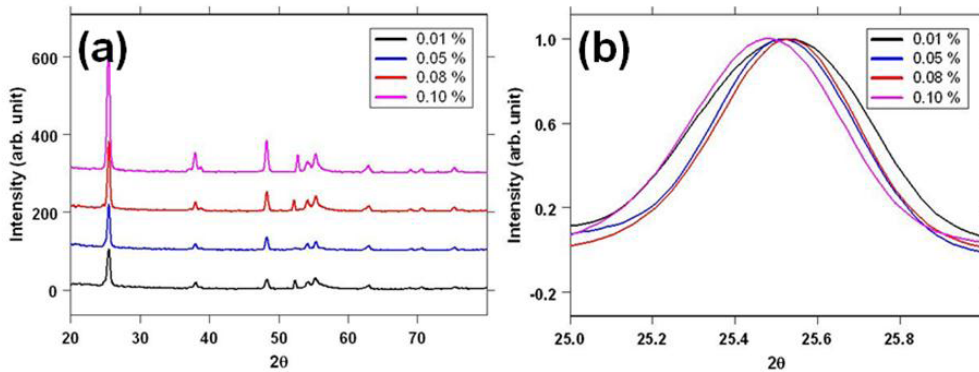


Fig. 3. XRD pattern of TiO₂-Pt thin film depends on Pt concentration.

$$D = 0.9\lambda / \beta \cos \theta$$

where λ is the X-ray wavelength of Copper K α radiation, θ is Bragg's angle and β is the pure full width of the diffraction line at half of the maximum intensity (Figure 3(b)). The calculated grain sizes are 15 nm (0.01%), 20 nm (0.05%), 35 nm (0.08%) and 40 nm (0.1%), separately. The result refers to that doping Pt also retard the grain growth of TiO₂ thin film.

AFM images of the Pt-TiO₂ surface were used to monitor the grain size of the sol-gel thin film depends on Pt concentration. 1 $\mu\text{m} \times 1 \mu\text{m}$ scans revealed it is clear that the grain size of Pt-TiO₂ gradually increased with Pt loading.

4 Conclusions

Metallic doping is one factor for TiO₂anatase phase grain growth. The intensity of the main anatase diffraction peak increased with increasing Pt concentration. The grain sizes estimated from anatase XRD major diffraction peaks were 15, 20, 35 and 40 nm for the sample with Pt concentration of 0.01%, 0.05%, 0.085 and 0.1%, respectively. The measured grain sizes using AFM images also increased depends on Pt concentration. The governing factor to determine the grain size of the TiO₂ thin films is Pt doping.

References

1. H. W. Wang, C.F. Ting, M.K. Hung, C.H. Chiou, Y.L. Liu, Z. Liu, K.R. Ratinac, S.P. Ringer, *Nanotechnology*, **20** (2009), pp. 055601.
2. J. Bai, B. Zhou, *Chem. Rev.* **114** (2014), pp. 10131.
3. V. Zoulalian, S. Monge, S. Zrcher, M. Textor, J.J. Robin, S. Tosatti, *J. Phys. Chem. B*, **110** (2006), pp. 25603.
4. N.B. Chaure, A.K. Ray, R. Capan, *Semicond. Sci. Technol.* **20** (2005), pp. 788.
5. H. Yaghoubi, N. Taghavinia, E.K. Alamdari, *Surf. Coating Tech.* **25** (2010) pp. 1562.
6. Q. Li, K. Ali, S. Lulia, P. Christos, H. Xu, P. Themistoklis, *Scientific Reports*, **4** (2014), pp. 4522.
7. W. Zhang, S. Chen, S. Yu, Y. Yin, *J. Crystal Growth*, **308** (2007), pp. 122.
8. T. Ohno, K. Sarukawa, M. Matsumura, *New J. Chem.* **26** (2002), pp. 1167.
9. X.H. Yang, Z. Li, C. Sun, H.G. Yang, C. Li, *Chem. Mater.* **13** (2011), pp. 3486.
10. G. Fu, P.S. Vary, C. Lin, *J. Phys. Chem. B*, **109** (2005), pp. 8889.
11. H. Zhang, G. Chen, *Environ. Sci. Technol.* **43** (2009), pp. 2905.
12. D. Morris, Y. Dou, J. Rebane, C.E.J. Mitchell, R.G. Egdell, *Phys. Rev. B*, **61** (2000), pp. 13445.
13. M. Enachi, M. Guix, T. Braniste, V. Postolache, V. Ciobanu, V. Ursaki, O.G. Schmidt, I. Tiginyanu, *Surf. Eng. Appl. Electrochem.* **51** (2015), pp. 3.

14. W.Y. Park, G.H. Kim, J.Y. Seok, K.M. Kim, S.J. Song, M.H. Lee, C.S. Hwang, *Nanotechnology*, **21** (2010), pp. 195201.
15. D. Eder, M. Motta, A.H. Windle, *Nanotechnology*, **20** (2009) 055602.
16. H. Tada, F. Suzuki, S. Yoneda, S. Ito and H. Kobayashi, *Phys. Chem. Chem. Phys.*, **3** (2001), pp. 1376.
17. L. Ravichandran, K. Selvam, B. Krishnakumar, M.. Swaminathan, *J. Hazardous Mater*, **167** (2009), pp. 763-769.
18. H. Wang, Z. Wu, Y. Liu, Y. Wang, *Chemosphere*, **74** (2008), pp. 773-778.
19. M. Beghi, P. Chiurlo, L. Costa, M. Palladino, M.F. Pirini, *J. Non-cryst. Solids*, **145** (1992), pp. 175.